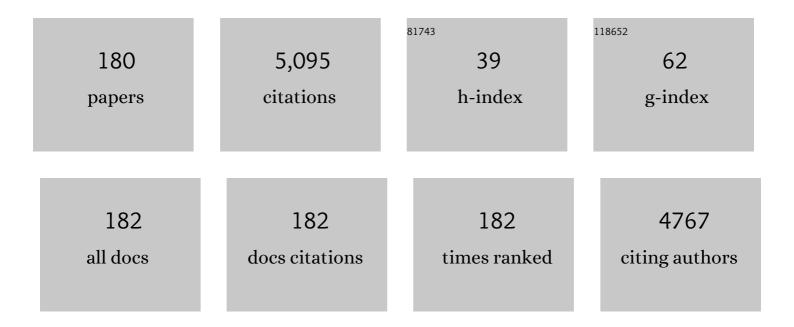
## Maximo Siu Li

List of Publications by Year in descending order

Source: https://exaly.com/author-pdf/1089978/publications.pdf Version: 2024-02-01



#	Article	IF	CITATIONS
1	Effect of Different Solvent Ratios (Water/Ethylene Glycol) on the Growth Process of CaMoO <sub>4</sub> Crystals and Their Optical Properties. Crystal Growth and Design, 2010, 10, 4752-4768.	1.4	204
2	Electronic structure, growth mechanism and photoluminescence of CaWO <sub>4</sub> crystals. CrystEngComm, 2012, 14, 853-868.	1.3	200
3	Morphology and Blue Photoluminescence Emission of PbMoO <sub>4</sub> Processed in Conventional Hydrothermal. Journal of Physical Chemistry C, 2009, 113, 5812-5822.	1.5	171
4	Cluster Coordination and Photoluminescence Properties of α-Ag <sub>2</sub> WO <sub>4</sub> Microcrystals. Inorganic Chemistry, 2012, 51, 10675-10687.	1.9	168
5	Electronic structure and optical properties of BaMoO4 powders. Current Applied Physics, 2010, 10, 614-624.	1.1	150
6	Experimental and Theoretical Investigations of Electronic Structure and Photoluminescence Properties of β-Ag <sub>2</sub> MoO <sub>4</sub> Microcrystals. Inorganic Chemistry, 2014, 53, 5589-5599.	1.9	133
7	Hierarchical Assembly of CaMoO <sub>4</sub> Nano-Octahedrons and Their Photoluminescence Properties. Journal of Physical Chemistry C, 2011, 115, 5207-5219.	1.5	130
8	Synthesis of wurtzite ZnS nanoparticles using the microwave assisted solvothermal method. Journal of Alloys and Compounds, 2013, 556, 153-159.	2.8	105
9	Structural refinement, optical and microwave dielectric properties of BaZrO3. Ceramics International, 2012, 38, 2129-2138.	2.3	104
10	Zinc blende versus wurtzite ZnS nanoparticles: control of the phase and optical properties by tetrabutylammonium hydroxide. Physical Chemistry Chemical Physics, 2014, 16, 20127-20137.	1.3	100
11	A relationship between structural and electronic order–disorder effects and optical properties in crystalline TiO <sub>2</sub> nanomaterials. Dalton Transactions, 2015, 44, 3159-3175.	1.6	96
12	Optical and dielectric relaxor behaviour of Ba(Zr <sub>0.25</sub> Ti <sub>0.75</sub> )O <sub>3</sub> ceramic explained by means of distorted clusters. Journal Physics D: Applied Physics, 2009, 42, 175414.	1.3	93
13	Structure and optical properties of [Ba1–xY2x/3](Zr0.25Ti0.75)O3 powders. Solid State Sciences, 2010, 12, 1160-1167.	1.5	84
14	Presence of excited electronic state in CaWO4 crystals provoked by a tetrahedral distortion: An experimental and theoretical investigation. Journal of Applied Physics, 2011, 110, .	1.1	84
15	A combined theoretical and experimental study of electronic structure and optical properties of β-ZnMoO4 microcrystals. Polyhedron, 2013, 54, 13-25.	1.0	83
16	Microstructure, dielectric properties and optical band gap control on the photoluminescence behavior of Ba[Zr0.25Ti0.75]O3 thin films. Journal of Sol-Gel Science and Technology, 2009, 49, 35-46.	1.1	81
17	Structural refinement, growth process, photoluminescence and photocatalytic properties of (Ba1-xPr2x/3)WO4 crystals synthesized by the coprecipitation method. RSC Advances, 2012, 2, 6438.	1.7	79
18	Intense blue and green photoluminescence emissions at room temperature in barium zirconate powders. Journal of Alloys and Compounds, 2009, 471, 253-258.	2.8	69

#	Article	IF	CITATIONS
19	β-ZnMoO4 microcrystals synthesized by the surfactant-assisted hydrothermal method: Growth process and photoluminescence properties. Colloids and Surfaces A: Physicochemical and Engineering Aspects, 2012, 396, 346-351.	2.3	66
20	Structural refinement, growth mechanism, infrared/Raman spectroscopies and photoluminescence properties of PbMoO4 crystals. Polyhedron, 2013, 50, 532-545.	1.0	63
21	Identifying and rationalizing the morphological, structural, and optical properties of <i><sup>2</sup></i> -Ag <sub>2</sub> MoO <sub>4</sub> microcrystals, and the formation process of Ag nanoparticles on their surfaces: combining experimental data and first-principles calculations. Science and Technology of Advanced Materials. 2015. 16. 065002.	2.8	61
22	Structural evolution, growth mechanism and photoluminescence properties of CuWO4 nanocrystals. Ultrasonics Sonochemistry, 2017, 38, 256-270.	3.8	60
23	White photoluminescence emission from ZrO2 co-doped with Eu3+, Tb3+ and Tm3+. Journal of Alloys and Compounds, 2016, 674, 245-251.	2.8	58
24	Blue-green and red photoluminescence in CaTiO3:Sm. Journal of Luminescence, 2007, 126, 403-407.	1.5	53
25	Urea-Based Synthesis of Zinc Oxide Nanostructures at Low Temperature. Journal of Nanomaterials, 2012, 2012, 1-7.	1.5	53
26	EPR, optical absorption and luminescence studies of Cr3+-doped antimony phosphate glasses. Optical Materials, 2014, 38, 119-125.	1.7	53
27	Optical and ESR study ofEr3+inLiNbO3. Physical Review B, 1995, 51, 3206-3209.	1.1	52
28	Intense violet–blue photoluminescence in BaZrO3 powders: A theoretical and experimental investigation of structural order–disorder. Optics Communications, 2008, 281, 3715-3720.	1.0	52
29	Structural evolution of Eu-doped hydroxyapatite nanorods monitored by photoluminescence emission. Journal of Alloys and Compounds, 2012, 531, 50-54.	2.8	50
30	Photoluminescent properties of ZrO2: Tm3+, Tb3+, Eu3+ powders—A combined experimental and theoretical study. Journal of Alloys and Compounds, 2017, 695, 3094-3103.	2.8	50
31	SnO2 nanocrystals synthesized by microwave-assisted hydrothermal method: towards a relationship between structural and optical properties. Journal of Nanoparticle Research, 2012, 14, 1.	0.8	49
32	Rietveld refinement, morphology and optical properties of (Ba <sub>1â^'<i>x</i></sub> Sr <i><sub>x</sub></i> )MoO <sub>4</sub> crystals. Journal of Applied Crystallography, 2013, 46, 1434-1446.	1.9	49
33	Synthesis of (Ca,Nd)TiO3 powders by complex polymerization, Rietveld refinement and optical properties. Spectrochimica Acta - Part A: Molecular and Biomolecular Spectroscopy, 2009, 74, 1050-1059.	2.0	48
34	An Experimental and Computational Study of β-AgVO <sub>3</sub> : Optical Properties and Formation of Ag Nanoparticles. Journal of Physical Chemistry C, 2016, 120, 12254-12264.	1.5	48
35	Understanding the White-Emitting CaMoO <sub>4</sub> Co-Doped Eu <sup>3+</sup> , Tb <sup>3+</sup> , and Tm <sup>3+</sup> Phosphor through Experiment and Computation. Journal of Physical Chemistry C, 2019, 123, 18536-18550.	1.5	45
36	Photoluminescence property of powders prepared by solid state reaction and polymeric precursor method. Physica B: Condensed Matter, 2009, 404, 3341-3347.	1.3	44

#	Article	IF	CITATIONS
37	Hierarchical growth of ZnO nanorods over SnO <sub>2</sub> seed layer: insights into electronic properties from photocatalytic activity. RSC Advances, 2016, 6, 2112-2118.	1.7	44
38	Off-CenterCu+Ions in Potassium Halides Studied with Ionic Thermocurrents. Physical Review B, 1973, 7, 4677-4682.	1.1	42
39	Structural Refinement and Photoluminescence Properties of MnWO4 Nanorods Obtained by Microwave-Hydrothermal Synthesis. Journal of Inorganic and Organometallic Polymers and Materials, 2012, 22, 264-271.	1.9	41
40	Investigation of structural and optical properties of CaTiO3 powders doped with Mg2+ and Eu3+ ions. Journal of Alloys and Compounds, 2015, 647, 265-275.	2.8	36
41	Structural properties and self-activated photoluminescence emissions in hydroxyapatite with distinct particle shapes. Ceramics International, 2018, 44, 236-245.	2.3	36
42	Effect of different surfactants on the shape, growth and photoluminescence behavior of MnWO4 crystals synthesized by the microwave-hydrothermal method. Advanced Powder Technology, 2012, 23, 124-128.	2.0	35
43	A new processing method of CaZn2(OH)6·2H2O powders: Photoluminescence and growth mechanism. Solid State Sciences, 2009, 11, 2173-2179.	1.5	34
44	Structure, morphology and photoluminescence emissions of ZnMoO4: RE 3+=Tb3+ - Tm3+ - X Eu3+ (xÂ= 1,) <sup>-</sup> Compounds, 2018, 750, 55-70.	Tj ETQq0 0 0 2.8	rgBT /Overloc 34
45	Preparation and photoluminescence characteristics of In(OH)3:xTb3+ obtained by Microwave-Assisted Hydrothermal method. Journal of Alloys and Compounds, 2013, 553, 338-342.	2.8	32
46	Effect of partial preferential orientation and distortions in octahedral clusters on the photoluminescence properties of FeWO4 nanocrystals. CrystEngComm, 2012, 14, 7127.	1.3	31
47	Local electronic structure, optical bandgap and photoluminescence (PL) properties of Ba(Zr0.75Ti0.25)O3 powders. Materials Science in Semiconductor Processing, 2013, 16, 1035-1045.	1.9	31
48	Effect of process parameters on photophysical properties and barium molybdate phosphors characteristics. Ceramics International, 2014, 40, 6719-6729.	2.3	31
49	Correlation between structural and electronic order–disorder effects and optical properties in ZnO nanocrystals. Journal of Materials Chemistry C, 2014, 2, 10164-10174.	2.7	31
50	Crystal growth and photoluminescence of europium-doped strontium titanate prepared by a microwave hydrothermal method. Ceramics International, 2015, 41, 3549-3554.	2.3	31
51	Electron scattering and effects of sources of light on photoconductivity of SnO2 coatings prepared by sol–gel. Journal of Non-Crystalline Solids, 1999, 247, 171-175.	1.5	30
52	Photoluminescent behavior of SrZrO3/SrTiO3 multilayer thin films. Chemical Physics Letters, 2009, 473, 293-298.	1.2	30
53	Above bandgap induced photoexpansion and photobleaching in Ga–Ge–S based glasses. Journal of Non-Crystalline Solids, 2001, 284, 282-287.	1.5	29
54	Electrosteric colloidal stabilization for obtaining SrTiO3/TiO2 heterojunction: Microstructural evolution in the interface and photonics properties. Journal of the European Ceramic Society, 2018, 38, 1621-1631.	2.8	29

#	Article	IF	CITATIONS
55	Growth process and grain boundary defects in Er doped BaTiO3 processed by EB-PVD: A study by XRD, FTIR, SEM and AFM. Applied Surface Science, 2019, 493, 982-993.	3.1	29
56	Indium hydroxide nanocubes and microcubes obtained by microwave-assisted hydrothermal method. Journal of Alloys and Compounds, 2010, 497, L25-L28.	2.8	28
57	Improved photoluminescence emission and gas sensor properties of ZnO thin films. Ceramics International, 2016, 42, 13555-13561.	2.3	28
58	Synthesis and characterization of Ag+ and Zn2+ co-doped CaWO4 nanoparticles by a fast and facile sonochemical method. Journal of Alloys and Compounds, 2020, 823, 153617.	2.8	28
59	The influence of oxygen in the photoexpansion of GaGeS glasses. Applied Surface Science, 2003, 205, 143-150.	3.1	27
60	Joint Experimental and Theoretical Analysis of Orderâ^'Disorder Effects in Cubic BaZrO <sub>3</sub> Assembled Nanoparticles under Decaoctahedral Shape. Journal of Physical Chemistry A, 2011, 115, 4482-4490.	1.1	27
61	Near-infrared light emission of Er3+-doped zirconium oxide thin films: An optical, structural and XPS study. Journal of Alloys and Compounds, 2015, 619, 800-806.	2.8	27
62	Photoluminescence properties of (Eu, Tb, Tm) co-doped PbMoO4 obtained by sonochemical synthesis. Journal of Alloys and Compounds, 2017, 700, 130-137.	2.8	27
63	Luminescence and structure of Er3+ doped Zirconia films deposited by electron beam evaporation. Thin Solid Films, 2002, 418, 222-227.	0.8	26
64	Optical multi-sites of Nd3+-doped CaMoO4induced by Nb5+charge compensator. Journal of Physics Condensed Matter, 2006, 18, 7883-7892.	0.7	26
65	Effect of different strontium precursors on the growth process and optical properties of SrWO4 microcrystals. Journal of Materials Science, 2015, 50, 8089-8103.	1.7	26
66	Light-induced relief gratings and a mechanism of metastable light-induced expansion in chalcogenide glasses. Physical Review B, 2001, 63, .	1.1	24
67	Structural characterization and photoluminescence behavior of pure and doped potassium strontium niobates ceramics with tetragonal tungsten–bronze structure. Ceramics International, 2016, 42, 4709-4714.	2.3	24
68	A novel approach to obtain highly intense self-activated photoluminescence emissions in hydroxyapatite nanoparticles. Journal of Solid State Chemistry, 2017, 249, 64-69.	1.4	24
69	Title is missing!. Journal of Sol-Gel Science and Technology, 1998, 13, 793-798.	1.1	23
70	Improved laser-heated pedestal growth system for crystal growth in medium and high isostatic pressure environment. Review of Scientific Instruments, 1999, 70, 4606-4608.	0.6	23
71	Very Intense Distinct Blue and Red Photoluminescence Emission in MgTiO <sub>3</sub> Thin Films Prepared by the Polymeric Precursor Method: An Experimental and Theoretical Approach. Journal of Physical Chemistry C, 2012, 116, 15557-15567.	1.5	23
72	One-step synthesis of CaMoO4: Eu3+ nanospheres by ultrasonic spray pyrolysis. Journal of Materials Science: Materials in Electronics, 2017, 28, 16867-16879.	1,1	23

#	Article	IF	CITATIONS
73	Influence of microwave-assisted hydrothermal treatment time on the crystallinity, morphology and optical properties of ZnWO4 nanoparticles: Photocatalytic activity. Ceramics International, 2020, 46, 1766-1774.	2.3	23
74	A joint experimental and theoretical study on the electronic structure and photoluminescence properties of Al2(WO4)3 powders. Journal of Molecular Structure, 2015, 1081, 381-388.	1.8	22
75	α- and β-AgVO3 polymorphs as photoluminescent materials: An example of temperature-driven synthesis. Ceramics International, 2018, 44, 5939-5944.	2.3	21
76	Photoreflectance measurements on Si Î′â€doped GaAs samples grown by molecularâ€beam epitaxy. Journal of Applied Physics, 1990, 67, 4149-4151.	1.1	20
77	Towards controlled synthesis and better understanding of blue shift of the CaS crystals. Journal of Materials Chemistry C, 2014, 2, 2743.	2.7	20
78	Influence of variables on the synthesis of CoFe2O4 pigment by the complex polymerization method. Journal of Advanced Ceramics, 2015, 4, 135-141.	8.9	20
79	Photoluminescence and photocatalytic properties of Ag/AgCl synthesized by sonochemistry: statistical experimental design. Journal of Materials Science: Materials in Electronics, 2017, 28, 12273-12281.	1.1	20
80	White light emission from single-phase Y2MoO6: xPr3+ (xÂ= 1, 2, 3 and 4â€ <sup>-</sup> mol%) phosphor. Journal of Alloys and Compounds, 2018, 769, 420-429.	2.8	20
81	Characterization of the structural, optical, photocatalytic and <i>in vitro</i> and <i>in vivo</i> anti-inflammatory properties of Mn <sup>2+</sup> doped Zn <sub>2</sub> GeO <sub>4</sub> nanorods. Journal of Materials Chemistry C, 2019, 7, 8216-8225.	2.7	20
82	An investigation into the influence of zinc precursor on the microstructural, photoluminescence, and gas-sensing properties of ZnO nanoparticles. Journal of Nanoparticle Research, 2014, 16, 1.	0.8	19
83	Growth mechanism and vibrational and optical properties of SrMoO4: Tb3+, Sm3+ particles: green–orange tunable color. Journal of Materials Science, 2020, 55, 8610-8629.	1.7	19
84	Photolumiscent Properties of Nanorods and Nanoplates Y2O3:Eu3+. Journal of Fluorescence, 2011, 21, 1431-1438.	1.3	18
85	Influence of the network modifier on the characteristics of MSnO3 (M=Sr and Ca) thin films synthesized by chemical solution deposition. Journal of Solid State Chemistry, 2013, 199, 34-41.	1.4	18
86	Effects of defects, grain size, and thickness on the optical properties of BaTiO3 thin films. Journal of Luminescence, 2017, 192, 969-974.	1.5	18
87	On the nature of the room temperature ferromagnetism in nanoparticulate co-doped ZnO thin films prepared by EB-PVD. Journal of Alloys and Compounds, 2017, 695, 2682-2688.	2.8	18
88	Computational Chemistry Meets Experiments for Explaining the Geometry, Electronic Structure, and Optical Properties of Ca <sub>10</sub> V <sub>6</sub> O <sub>25</sub> . Inorganic Chemistry, 2018, 57, 15489-15499.	1.9	18
89	Structural investigation and improvement of photoluminescence properties in Ba(ZrxTi1â^'x)O3 powders synthesized by the solid state reaction method. Materials Chemistry and Physics, 2013, 142, 70-76.	2.0	17
90	Optical properties of Nd3+-doped Ca3(VO4)2 single crystal fiber. Optical Materials, 2003, 22, 369-375.	1.7	16

#	Article	IF	CITATIONS
91	Spectroscopic study of Nd-doped amorphous SiN films. Journal of Applied Physics, 2004, 96, 1068-1073.	1.1	16
92	Evaluation of the OHâ^' influence on visible and near-infrared quantum efficiencies of Tm3+ and Yb3+ codoped sodium aluminophoshate glasses. Journal of Applied Physics, 2006, 100, 123103.	1.1	16
93	Luminescent and thermo-optical properties of Nd3+-doped yttrium aluminoborate laser glasses. Journal of Applied Physics, 2009, 106, .	1.1	16
94	Blue and red light photoluminescence emission at room temperature from CaTiO3 decorated with α-Ag2WO4. Ceramics International, 2017, 43, 5759-5766.	2.3	16
95	Activation energy and its fluctuations at grain boundaries of Er3+:BaTiO3 perovskite thin films: Effect of doping concentration and annealing temperature. Vacuum, 2021, 194, 110562.	1.6	16
96	Disclosing the electronic structure and optical properties of Ag <sub>4</sub> V <sub>2</sub> O <sub>7</sub> crystals: experimental and theoretical insights. CrystEngComm, 2016, 18, 6483-6491.	1.3	15
97	Photoinduced structural changes in antimony polyphosphate based glasses. Journal of Non-Crystalline Solids, 2003, 330, 168-173.	1.5	14
98	Red shift and higher photoluminescence emission of CCTO thin films undergoing pressure treatment. Journal of Alloys and Compounds, 2014, 583, 488-491.	2.8	14
99	High red emission intensity of Eu:Y2O3 films grown on Si(1 0 0)/Si(1 1 1) by electron beam evaporation. Journal of Luminescence, 2014, 148, 186-191.	1.5	14
100	Influence Ca-doped SrIn2O4 powders on photoluminescence property prepared one step by ultrasonic spray pyrolysis. Journal of Alloys and Compounds, 2018, 747, 1078-1087.	2.8	14
101	Designing biocompatible and multicolor fluorescent hydroxyapatite nanoparticles for cell-imaging applications. Materials Today Chemistry, 2019, 14, 100211.	1.7	14
102	Annealing effects on optical properties of natural alexandrite. Journal of Physics Condensed Matter, 2003, 15, 7437-7443.	0.7	12
103	Photo-induced effects in Ge25Ga10S65 glasses studied by XPS and XAS. Solid State Ionics, 2005, 176, 1403-1409.	1.3	11
104	Energy transfer processes in Yb <sup>3+</sup> –Tm <sup>3+</sup> co-doped sodium alumino-phosphate glasses with improved 1.8 µm emission. Journal of Physics Condensed Matter, 2008, 20, 255240.	0.7	11
105	Formation of $\hat{I}^2$ -nickel hydroxide plate-like structures under mild conditions and their optical properties. Journal of Solid State Chemistry, 2011, 184, 2818-2823.	1.4	11
106	Structure, morphology, and optical properties of (Ca1â^'3x Eu2x )WO4 microcrystals. Electronic Materials Letters, 2015, 11, 193-197.	1.0	11
107	Emission Properties Related to Distinct Phases of Sol-Gel Dip-Coating Titanium Dioxide, and Carrier Photo-Excitation in Different Energy Ranges. Materials Research, 2017, 20, 866-873.	0.6	11
108	Unveiling the efficiency of microwave-assisted hydrothermal treatment for the preparation of SrTiO <sub>3</sub> mesocrystals. Physical Chemistry Chemical Physics, 2019, 21, 22031-22038.	1.3	11

#	Article	IF	CITATIONS
109	Paraelastic Alignment and Electric Dipole Relaxation Behavior of Offâ€Center Ag <sup>+</sup> Defects in Rbl. Physica Status Solidi (B): Basic Research, 1981, 106, 683-692.	0.7	10
110	Influence of annealing on X-ray diffraction of natural alexandrite. Powder Diffraction, 2002, 17, 135-138.	0.4	10
111	Growth and evaluation of lanthanoids orthoniobates single crystals processed by a miniature pedestal growth technique. Crystal Research and Technology, 2004, 39, 859-863.	0.6	10
112	Spectroscopic study of floating zone technique-grown Nd3+-doped CaMoO4. EPJ Applied Physics, 2005, 29, 55-64.	0.3	10
113	Structural disorder-dependent upconversion in Er3+/Yb3+-doped calcium titanate. Ceramics International, 2014, 40, 15981-15984.	2.3	10
114	Effect of Er3+ concentration on the luminescence properties of Al2O3-ZrO2 powder. Optical Materials, 2016, 62, 553-560.	1.7	10
115	The extrinsic nature of double broadband photoluminescence from the BaTiO <sub>3</sub> perovskite: generation of white light emitters. Physical Chemistry Chemical Physics, 2021, 23, 18694-18706.	1.3	10
116	Structural study of thin films prepared from tungstate glass matrix by Raman and X-ray absorption spectroscopy. Applied Surface Science, 2008, 254, 5552-5556.	3.1	9
117	Blue or red photoluminescence emission in αâ€Bi 2 O 3 needles: Effect of synthesis method. Luminescence, 2018, 33, 1281-1287.	1.5	9
118	Red-emitting CaWO4:Eu3+,Tm3+ phosphor for solid-state lighting: Luminescent properties and morphology evolution. Journal of Rare Earths, 2022, 40, 226-233.	2.5	9
119	Photoinduced effect in Ga–Ge–S based thin films. Applied Surface Science, 2006, 252, 8738-8744.	3.1	8
120	Source of slow lithium atoms from Ne or H2matrix isolation sublimation. Journal of Chemical Physics, 2012, 136, 154202.	1.2	8
121	Structure, optical properties, and photocatalytic activity of α-Ag2W0.75Mo0.25O4. Materials Research Bulletin, 2020, 132, 111011.	2.7	8
122	570 nm and 4.8 μm emissions in Yb2+/CN- double doped KCl. Journal of Luminescence, 1994, 59, 289-291.	1.5	7
123	Dielectric Studies of CN? Dipolar Reorientation and Order/Disorder Behavior. Physica Status Solidi (B): Basic Research, 1997, 199, 245-264.	0.7	7
124	Photoluminescence spectrum of rare earth doped zirconia fibre and power excitation dependence. Radiation Effects and Defects in Solids, 1999, 149, 153-157.	0.4	7
125	Structural and optical characterization of beta barium borate thin films grown by electron beam evaporation. Journal of Vacuum Science and Technology A: Vacuum, Surfaces and Films, 2004, 22, 2163-2167.	0.9	7
126	Holographic recording in [Sb(PO3)3]n–Sb2O3 glassy films by photoinduced volume and refraction index changes. Journal of Non-Crystalline Solids, 2004, 348, 245-249.	1.5	7

#	Article	IF	CITATIONS
127	Thermal annealing-induced electric dipole relaxation in natural alexandrite. Physics and Chemistry of Minerals, 2005, 31, 733-737.	0.3	7
128	Thermo-optical characteristics and concentration quenching effects in Nd3+doped yttrium calcium borate glasses. Journal of Chemical Physics, 2011, 134, 124503.	1.2	7
129	Solvent effect on the optimization of 1.54Âμm emission in Er-doped Y2O3–Al2O3–SiO2 powders synthesized by a modified Pechini method. Current Applied Physics, 2013, 13, 1558-1565.	1.1	7
130	Effect of Zn2+ ions on the structure, morphology and optical properties of CaWO4 microcrystals. Journal of Sol-Gel Science and Technology, 2014, 72, 648-654.	1.1	7
131	Luminescence of Eu^3+ in the thin film heterojunction GaAs/SnO_2. Optical Materials Express, 2015, 5, 59.	1.6	7
132	MBE growth and characterization of δ-doping in GaAs and GaAs/Si. Surface Science, 1990, 228, 356-358.	0.8	6
133	Optical and structural characterizations of Cu+-doped KCl films. Thin Solid Films, 1994, 250, 273-278.	0.8	6
134	Effects of isostatic oxygen pressure on the crystal growth and optical properties of undoped and Er3+-doped Ca3(VO4)2 single-crystal Fibres. Advanced Materials for Optics and Electronics, 2000, 10, 9-15.	0.6	6
135	Colored films produced by electron beam deposition from nanometric TiO2 and Al2O3 pigment powders obtained by modified polymeric precursor method. Dyes and Pigments, 2007, 75, 693-700.	2.0	6
136	Thin films prepared from tungstate glass matrix. Applied Surface Science, 2008, 254, 2085-2089.	3.1	6
137	Photoluminescence of core–shell nanoparticles made from yttrium stabilized zirconia powder grain coated with alumina. CrystEngComm, 2013, 15, 3292.	1.3	6
138	Fast photocatalytic degradation of an organic dye and photoluminescent properties of Zn doped In(OH)3 obtained by the microwave-assisted hydrothermal method. Materials Science in Semiconductor Processing, 2014, 27, 1036-1041.	1.9	6
139	Matrix isolation sublimation: An apparatus for producing cryogenic beams of atoms and molecules. Review of Scientific Instruments, 2015, 86, 073109.	0.6	6
140	Enhanced red emission in Sr(1-x)EuxMo0.5W0.5O4 (x = 0.01, 0.02, 0.04) phosphor and spectroscopic analysis for display applications. Journal of Materials Science, 2022, 57, 8634-8647.	1.7	6
141	Off enter Cu <sup>+</sup> in mixed crystals. Physica Status Solidi (B): Basic Research, 1979, 92, 287-291.	0.7	5
142	Study of Ca2Fe2â^'xNbxO5+x phases by X-ray diffraction, IR and EPR spectroscopy. Materials Research Bulletin, 1992, 27, 523-529.	2.7	5
143	ITC study of Ga <sup>+</sup> -, Ge <sup>2+</sup> -, and Sn <sup>2+</sup> -doped alkali halides. Radiation Effects and Defects in Solids, 1998, 147, 11-16.	0.4	5
144	Raman spectroscopy analysis of structural photoinduced changes in GeS2+Ga2O3 thin films. Current Applied Physics, 2010, 10, 1411-1415.	1.1	5

#	Article	IF	CITATIONS
145	Optical characterization of europium-doped indium hydroxide nanocubes obtained by Microwave-Assisted Hydrothermal method. Materials Research, 2014, 17, 933-939.	0.6	5
146	Enhancement of symmetry-induced photoluminescence in bismuth tungstate microcrystals. Materials Letters, 2016, 184, 298-300.	1.3	5
147	Ionic Thermal Currents under Uniaxial Stress A New Method to Determine Electric and Elastic Dipole Properties. Physica Status Solidi (B): Basic Research, 1982, 112, 685-693.	0.7	4
148	Coupled Pairs of Cu <sup>+</sup> OCN <sup>â^'</sup> in KCl Studied by Optical Absorption and Thermally Stimulated Depolarization Current. Physica Status Solidi (B): Basic Research, 1992, 171, 141-151.	0.7	4
149	Strong and Broad 570 nm Emission in KCI: Yb <sup>2+</sup> :CN <sup>â^'</sup> . Physica Status Solidi (B): Basic Research, 1993, 180, K93.	0.7	4
150	Light-induced relaxing dipoles inn-typeAlxGa1â^'xAs. Physical Review B, 1995, 51, 13864-13867.	1.1	4
151	Photodesorption and electron trapping in n-type SnO <sub>2</sub> thin films grown by dip-coating technique. Radiation Effects and Defects in Solids, 1998, 146, 199-206.	0.4	4
152	On the upconversion emission of rare earth doped zirconia fiber. Radiation Effects and Defects in Solids, 1998, 147, 77-81.	0.4	4
153	Light-induced electric dipole relaxation in synthetic and natural alexandrite. Radiation Effects and Defects in Solids, 2001, 156, 295-299.	0.4	4
154	Local order around of germanium atoms in Ga10Ge25S65 glass by EXAFS. Journal of Non-Crystalline Solids, 2002, 304, 160-166.	1.5	4
155	Photoexpansion and photobleaching effects in oxysulfide thin films of the GeS2+Ga2O3 system. Physica B: Condensed Matter, 2011, 406, 4381-4386.	1.3	4
156	New insights into the nature of the bandgap of CuGeO3 nanofibers: Synthesis, electronic structure, and optical and photocatalytic properties. Materials Today Communications, 2021, 26, 101701.	0.9	4
157	Dipole relaxation current innâ€ŧype AlxGa1â^'xAs. Applied Physics Letters, 1993, 63, 2658-2660.	1.5	3
158	Off-center effect of Cu+-doped KC1 films studied by optical absorption and thermally stimulated depolarization current. Thin Solid Films, 1995, 268, 30-34.	0.8	3
159	Oxygen related defects excitation and photoconductivity dependence of SnO <sub>2</sub> Sol-Gel films with several light sources. Radiation Effects and Defects in Solids, 1999, 150, 391-395.	0.4	3
160	Two-dimensional photonic crystals in antimony-based films fabricated by holography. Journal of Applied Physics, 2008, 103, 106101.	1.1	3
161	Unraveling the Photoluminescence Properties of the Sr <sub>10</sub> V <sub>6</sub> O <sub>25</sub> Structure through Experimental and Theoretical Analyses. Journal of Physical Chemistry C, 2020, 124, 14446-14458.	1.5	3
162	Second harmonic generation and thermally stimulated depolarization current investigation of K1-XLiXTao3. Radiation Effects and Defects in Solids, 1995, 134, 229-232.	0.4	2

#	Article	IF	CITATIONS
163	Morphology and Optical Properties of SrWO4 Powders Synthesized by the Coprecipitation and Polymeric Precursor Methods. , 2017, , 131-154.		2
164	Facile Microwave-Assisted Synthesis of Lanthanide Doped CaTiO3Nanocrystals. Journal of the Brazilian Chemical Society, 2015, , .	0.6	2
165	Elasto- and electro-optical dipole properties of off-center Ag <sup>+</sup> defects in RbI. Radiation Effects, 1983, 73, 123-129.	0.4	1
166	Dipole Relaxation Current in N-Type AlxGa1-xAs. Materials Research Society Symposia Proceedings, 1993, 325, 285.	0.1	1
167	Thermally stimulated depolarization current of monovalent copper ions in calcium fluoride. Radiation Effects and Defects in Solids, 1995, 135, 121-123.	0.4	1
168	Ultraviolet and infrared spectroscopy of oh-/Cu+ double doped NaF. Radiation Effects and Defects in Solids, 1995, 133, 321-328.	0.4	1
169	CU <sup>+</sup> and OH <sup>â^'</sup> pairs defects interaction in NaF crystals. Radiation Effects and Defects in Solids, 1995, 134, 353-356.	0.4	1
170	Investigation of temperature influence on photo-induced conductivity in n-type AlxGa1â^'xAs. Radiation Effects and Defects in Solids, 1998, 146, 175-186.	0.4	1
171	Contribution of oxygen related defects to the electronic transport in SnO2sol-gel films. Radiation Effects and Defects in Solids, 2001, 156, 145-149.	0.4	1
172	Photoluminescence of the Eu-doped thin film heterojunction GaAs/SnO2 and rare-earth doping distribution. IOP Conference Series: Materials Science and Engineering, 2015, 76, 012006.	0.3	1
173	The role of the Tm <sup>3+</sup> concentration on CaMoO <sub>4</sub> properties processed by microwave hydrothermal under stirring condition. Journal of the American Ceramic Society, 2021, 104, 5192-5204.	1.9	1
174	SÃntese de BaTiO3 e SrTiO3 pelo método hidrotermal assistido por micro-ondas utilizando anatase como precursor de titânio. Quimica Nova, 0, , .	0.3	1
175	Continuous to bound interband transitions in δ-doped GaAs layers. Superlattices and Microstructures, 1990, 8, 205-208.	1.4	0
176	CU <sup>+</sup> high doping effects in KCl and KBr films. Radiation Effects and Defects in Solids, 1995, 134, 357-360.	0.4	0
177	Yb <sup>2+</sup> /CN <sup>â^'</sup> doped KBr absorption and emission structure. Radiation Effects and Defects in Solids, 1998, 146, 349-355.	0.4	0
178	Study of KCl + <i>x</i> % in and KCl + <i>y</i> % tici thin films. Radiation Effects and Defects in Solids, 1998, 147, 83-91.	0.4	0
179	Analysis of the topography of a Bragg grating in chalcogenide glass. Applied Surface Science, 2001, 181, 19-27.	3.1	0
180	CoO doping effects on the ZnO films through EBPDV technique. EPJ Applied Physics, 2014, 65, 30301.	0.3	0